Institute of High Energy Physics
Chinese Academy of Sciences

Pulsar Polarization Arrays

Jing Ren (任婧)

中科院高能所理论室 (TPD, IHEP)

First International Conference on Axion Physics and Experiment (Axion 2022)

November 23, 2022

Based on work with Tao Liu, Xuzixiang Lou, arXiv: 2111.10615

Content

- ✦ Pulsar timing arrays (PTAs) and pulsar polarization arrays (PPAs)
- ✦ Ultralight axion-like dark matter (ALDM)
- ✦ Ultralight ALDM detection by PPAs through cosmic birefringence

Pulsars

- Pulsars emit electromagnetic pulses with extraordinary regularity, with the period ranging from milliseconds to seconds. Up to now about 3000 pulsars observed in our galaxy
- Millisecond pulsars (MSPs) are especially stable due to mass and angular momentum transfer from a companion. Although emission mechanism not fully clarified, they play significant roles as astronomical clocks

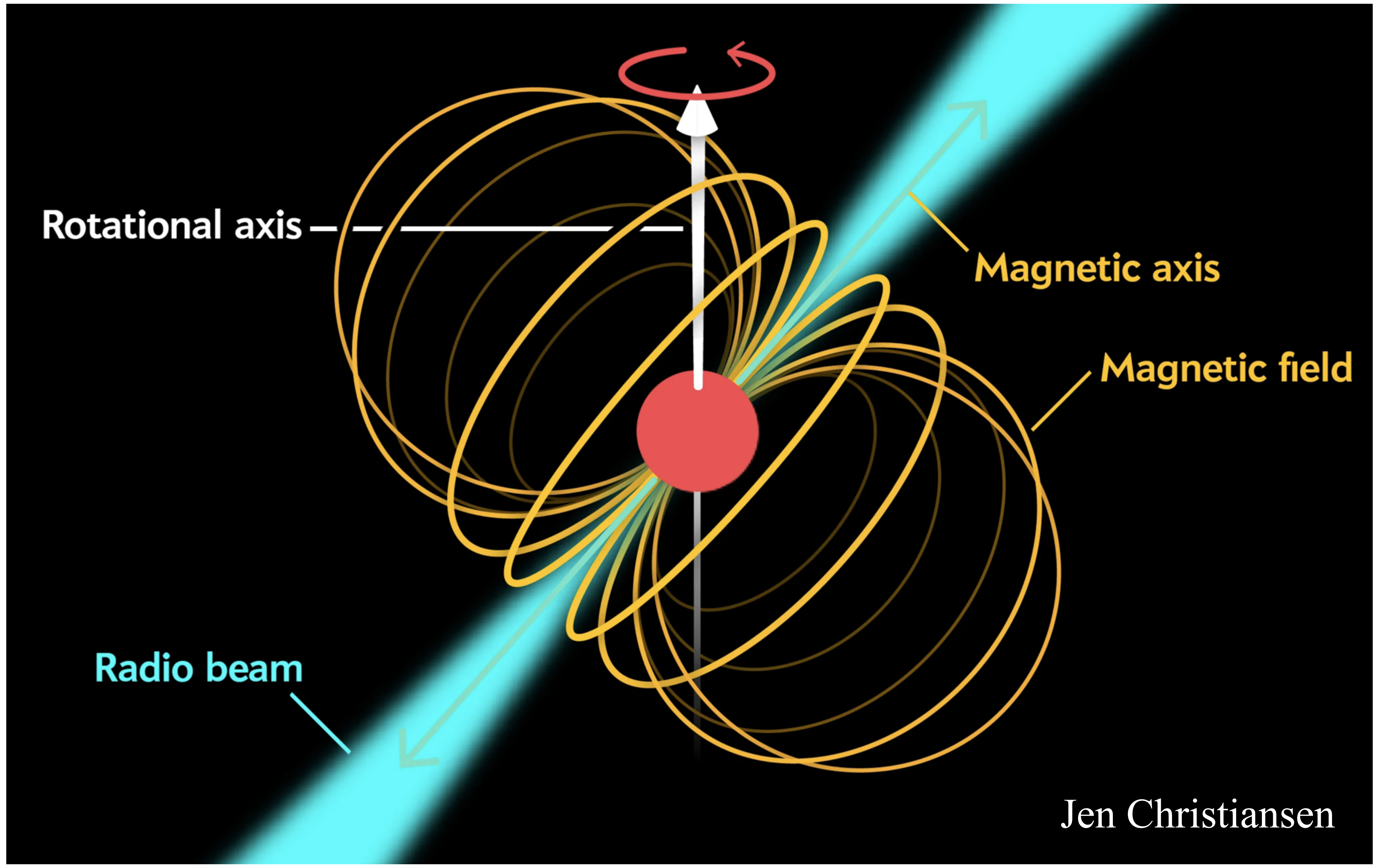

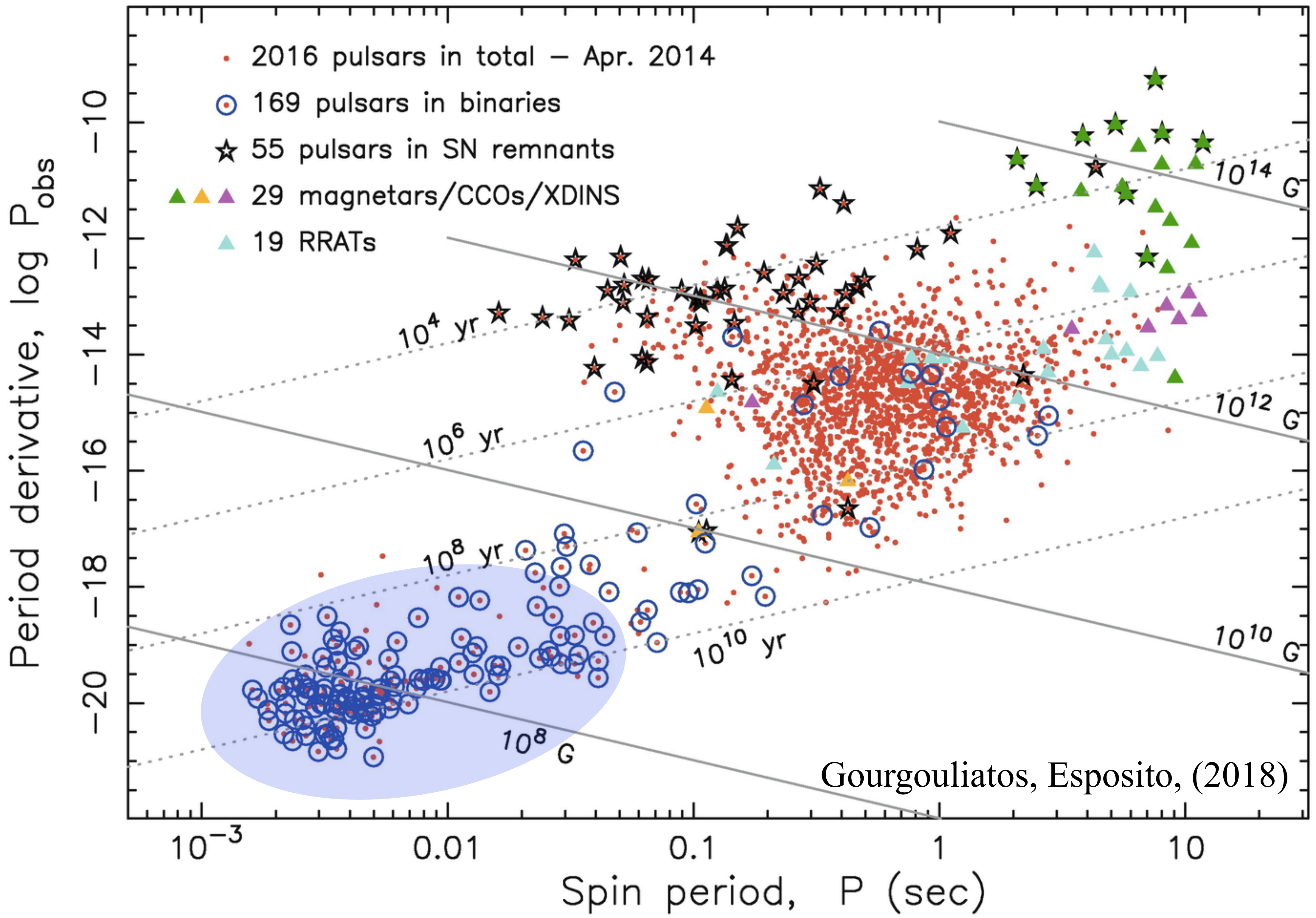

Pulsar timing arrays (PTAs)

- Global PTA network monitors over 80 MSPs in the timespan of years. FAST/SKA may increase the number to the order of 1000

- Given precise timing model of the expected time of arrival of the pulse, the measured **time difference** can be directly related to **gravitational waves (GWs)**

$$\Delta T(t) = \int_{-\infty}^{\infty} df \frac{1}{2} u^a u^b h_{ab}(f, \hat{n})\, e^{i2\pi f(t+\hat{n}\cdot\vec{r}_2/c)} \frac{1}{i2\pi f} \frac{1}{1+\hat{n}\cdot\hat{u}} \left[1 - e^{-\frac{i2\pi f L}{c}(1+\hat{n}\cdot\hat{u})}\right]$$

metric perturbation — "Earth" — "pulsar"

- PTAs with MSPs in different directions serve as **galactic interferometers** to measure nHZ GWs. Stochastic GW backgrounds (SGWBs) can be identified by the **quadrupolar spatial correlations among pulsars**

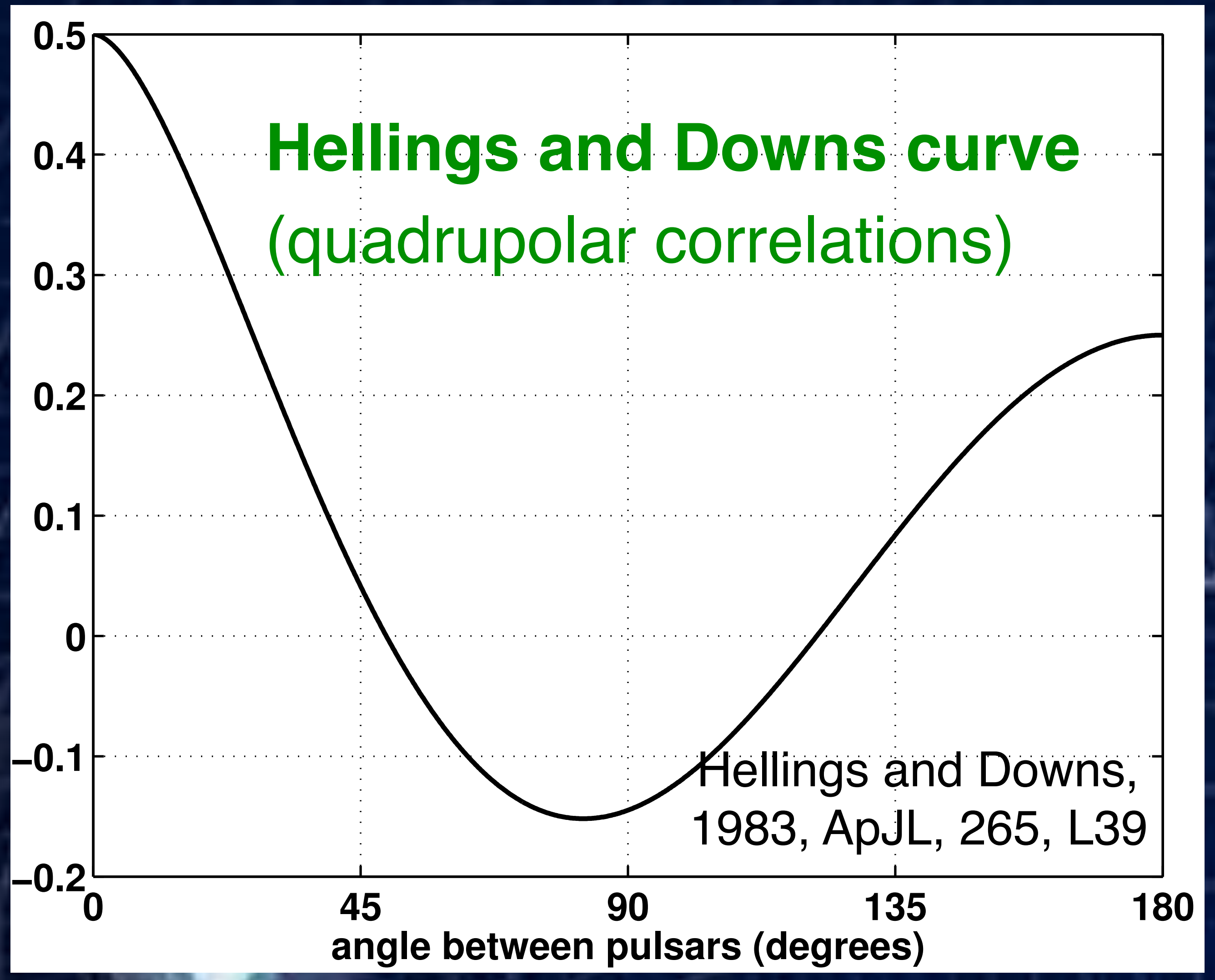

Pulsar timing arrays (PTAs)

Recently, the explorations on the PTA targets extended to dark matter (DM) physics

Oscillating gravitational potential induced by ultralight scalar DM

Khmelnitsky and Rubakov, 1309.5888; De Martino et al. 1705.04367; Porayko et al., 1810.03227

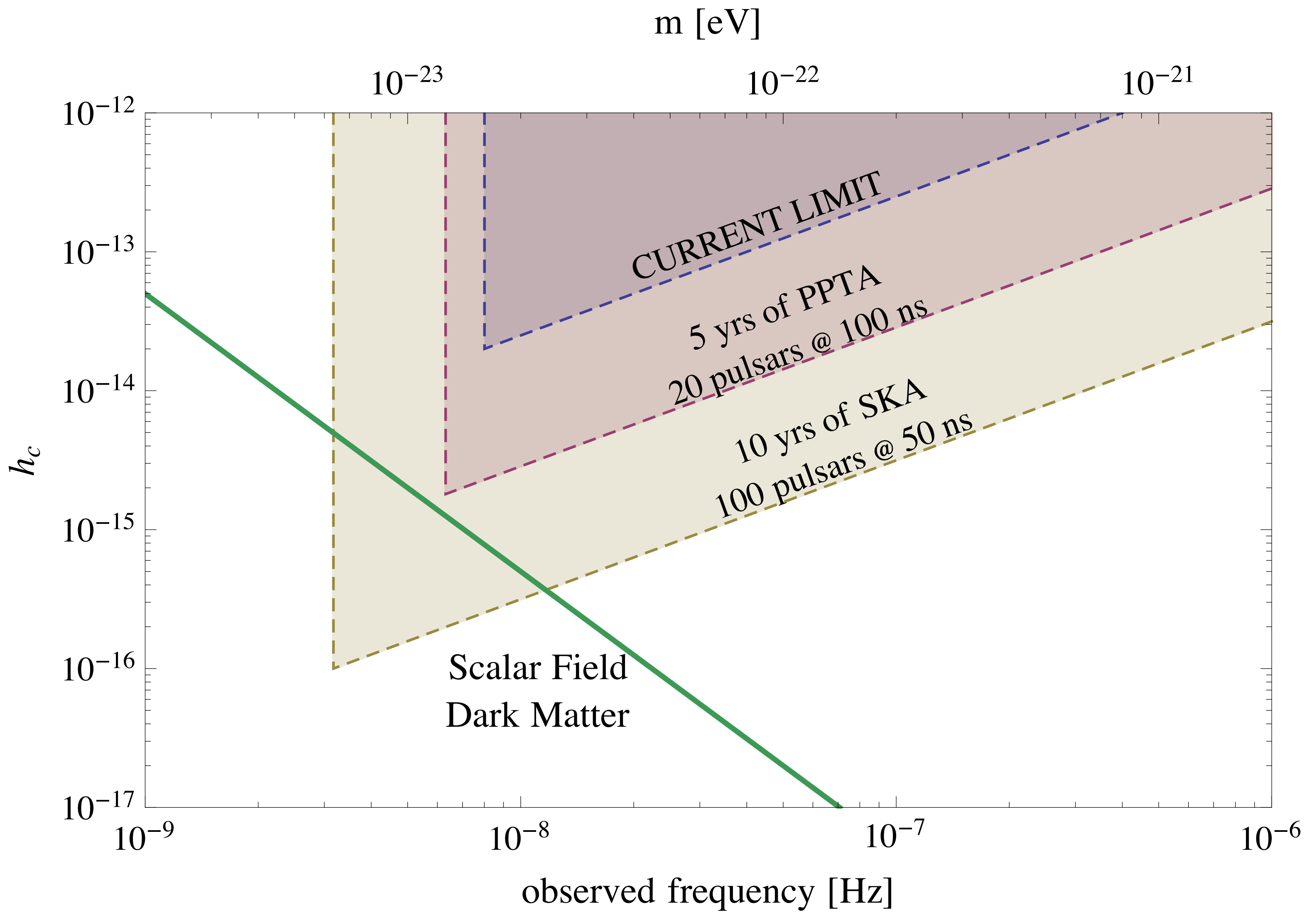

Doppler/Shapiro effects induced by transiting objects associated with DM substructure

Zurek et al., 1901.04490, 2005.03030, 2104.05717

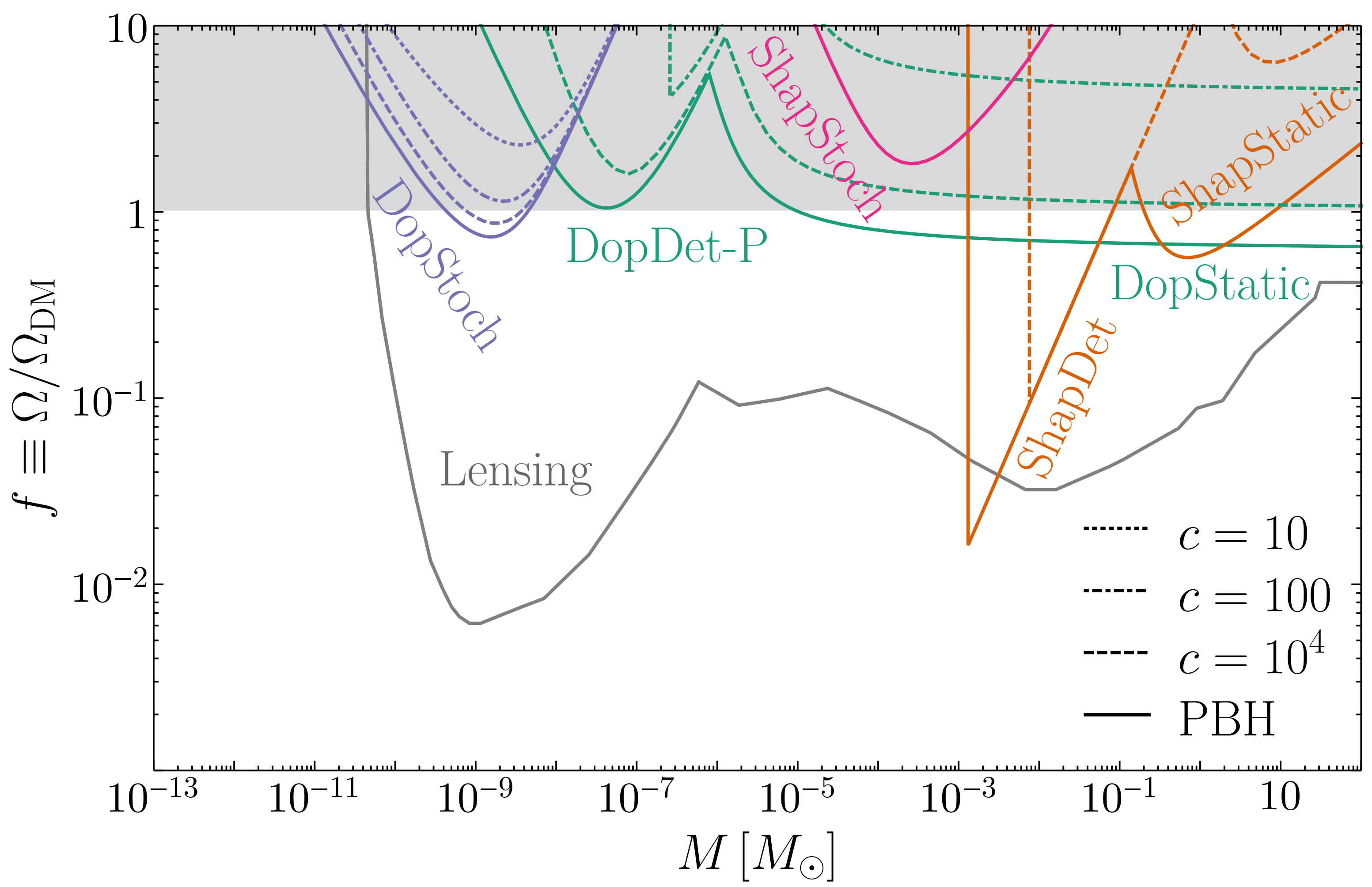

Oscillating fifth force induced by ultralight dark photon DM

Xue et al. [PPTA], 2112.07687

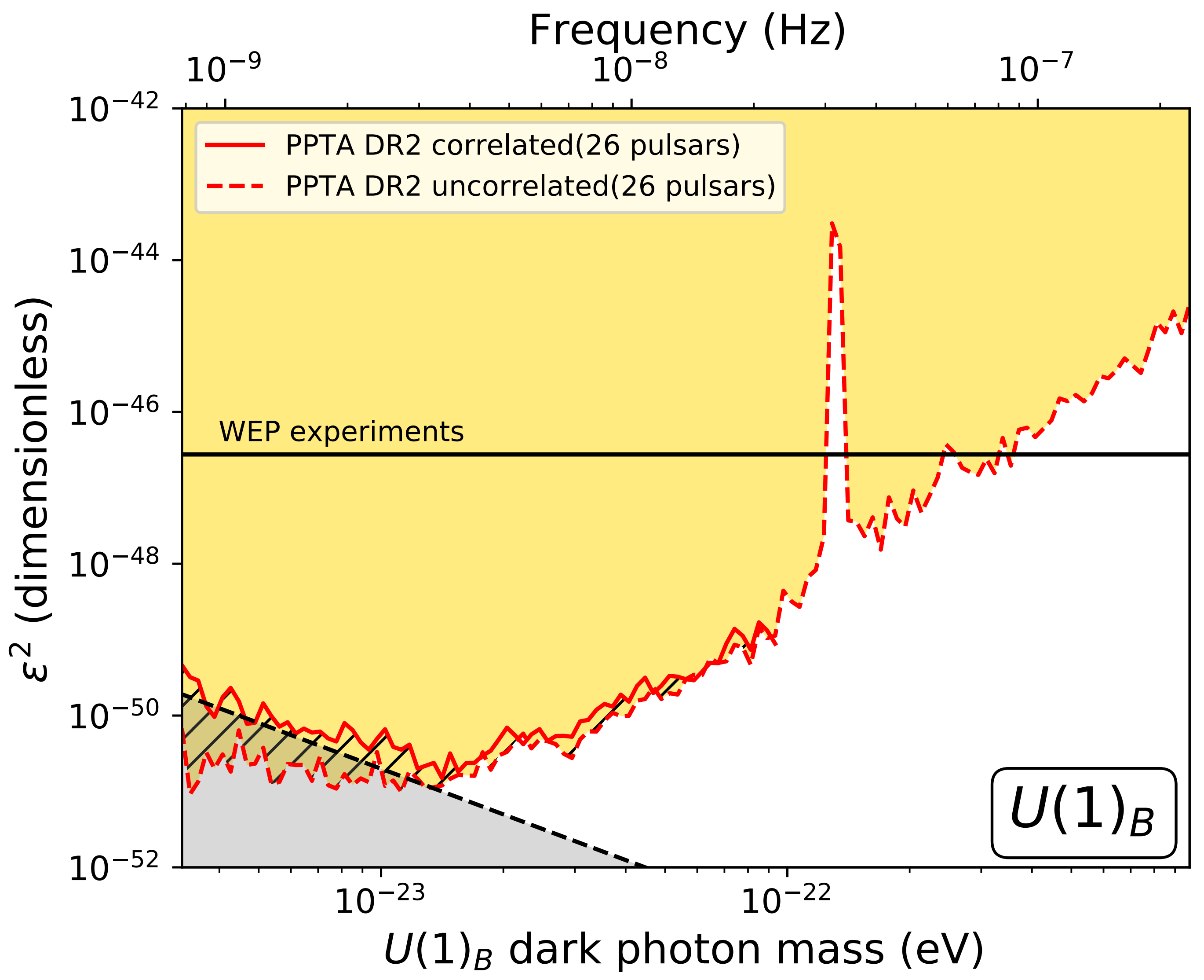

Pulsar polarization arrays (PPAs)

- Pulsar radio emissions typically have strong linear polarization

#	NAME		P0 (s)			DM (cm^-3 pc)			RM (rad m^-2)			DIST (kpc)
1	J0002+6216	cwp+17	0.1153635682680	14	cwp+17	218.6	6	wcp+18	*	0	*	6.357
2	J0006+1834	cnt96	0.69374767047	14	cn95	11.41	55	bkk+16	-20	3	npn+20	0.860
3	J0007+7303	aaa+09c	0.3158731909	3	awd+12	*	0	*	*	0	*	1.400
4	J0011+08	dsm+16	2.55287	0	dsm+16	24.9	0	dsm+16	*	0	*	5.399
5	B0011+47	dth78	1.240699038946	11	hlk+04	30.405	13	bkk+16	-15.56	10	sbg+19	1.776
36	J0026+6320	jml+09	0.31835777079	3	sjm+19	245.06	6	sjm+19	-294	2	npn+20	6.619
37	J0030+0451	lzb+00	0.0048654532114961	19	aab+21a	4.332772	0	aab+21a	1.17	8	sbg+19	0.324
38	J0033+57	hrk+08	0.315	0	hrk+08	75.65	9	mss+20	*	0	*	2.251
39	J0033+61	hrk+08	0.912	0	hrk+08	37.7	3	mss+20	*	0	*	1.654
40	J0034-0534	bhl+94	0.0018771818845850	2	aaa+10b	13.76517	4	aaa+10b	-38	17	hmvd18	1.348
96	B0144+59	stwd85	0.19632137543003	16	ywml10	40.111	3	hlk+04	-9.5	5	npn+20	2.128
97	B0148-06	mlt+78	1.464664549334	7	hlk+04	25.66	3	hlk+04	2	4	hl87	25.000
98	J0152+0948	clm+05	2.74664729014	10	clm+05	22.881	12	bkk+16	1.4	2	sbg+19	2.477
99	B0149-16	mlt+78	0.8327416126878	13	hlk+04	11.92577	4	srb+15	+6.6	50	fdr15	0.920
100	J0154+1833	mgf+19	0.0023645697763006	5	mgf+19	19.7978	1	mgf+19	21.6	1	mgf+19	1.622
366	J0818-3232	bjd+06	2.161258926939	15	bjd+06	131.80	7	bjd+06	25.2	50	hmvd18	0.484
367	B0818-13	vl70	1.2381295438682	8	hlk+04	40.938	3	hlk+04	-1.2	4	hl87	1.900
368	J0820-3826	bkl+13	0.1248366735581	5	psj+19	195.50	3	mss+20	+122	6	jsd+21	4.084
369	J0820-3921	bjd+06	1.07356658405	4	bjd+06	179.4	1	bjd+06	126.9	71	hmvd18	3.576
370	B0818-41	mlt+78	0.5454455601	3	lbs+20	113.4	2	antt94	57.7	5	qmlg95	0.571

ATNF Pulsar Catalogue
(Version: 1.66)

$$\mathrm{RM} = \frac{\mathrm{PA}}{\lambda^2}$$

rotation measure · polarization angle · wavelength

- Polarization profiles are usually obtained as a by-product of PTAs due to the crucial role played by polarization calibration for precise timing arXiv > astro-ph > arXiv:2111.10615

Search...

Help | Adva

Astrophysics > High Energy Astrophysical Phenomena

[Submitted on 20 Nov 2021]

Pulsar Polarization Arrays

Tao Liu, Xuzixiang Lou, Jing Ren

Pulsar timing arrays (PTAs) consisting of widely distributed and well-timed millisecond pulsars can serve as a galactic interferometer to measure gravitational waves. With the same data acquired for PTAs, we propose to develop pulsar polarization arrays (PPAs), to explore astrophysics and fundamental physics. As in the case of PTAs, PPAs are best suited to reveal temporal and spatial correlations at large scales that are hard to mimic by local noise. To demonstrate the physical potential of PPAs, we consider detection of ultralight axion-like dark matter (ALDM), through cosmic birefringence induced by its Chern-Simon coupling. Because of its tiny mass, the ultralight ALDM can be generated as a Bose-Einstein condensate, characterized by a strong wavy nature. Incorporating both temporal and spatial correlations of the signal, we show that PPAs have a potential to probe the Chern-Simon coupling up to $\sim 10^{-14} - 10^{-17}\text{GeV}^{-1}$, with a mass range $\sim 10^{-27} - 10^{-21}$eV.

Measured polarization angle:

$$\text{PA} = \text{PA}_{\text{source}} + \text{PA}_{\text{instru}} + \text{PA}_{\text{propa}}$$

- **Source**: change of pulsar orientation/magnetosphere; stochastic variation of single pulse profile (jitter noise)
- **Instrument**: related to PA calibration; radiometer noise
- **Propagation**: Faraday rotation caused by interstellar magnetic field/Earth's ionosphere

New physics effects??

Axion and axion-like particles (ALPs)

- **QCD axion** well motivated to solve the strong CP problem and also serve as an DM candidate; **ALPs** introduced in many BSM scenarios, e.g. string axions.

- **Ultralight ALPs** ($m_a < 10^{-18}$eV) can be generated as a Bose-Einstein condensate from misalignment; behave effectively as a **classical scalar field**

- **Ultralight ALPs may serve as DM or DE during cosmic evolution**. Here we focus on ALDM (e.g. fuzzy DM at $m_a \sim 10^{-22}$eV, subdominant at $m_a < 10^{-24}$eV)

ALPs landscapes

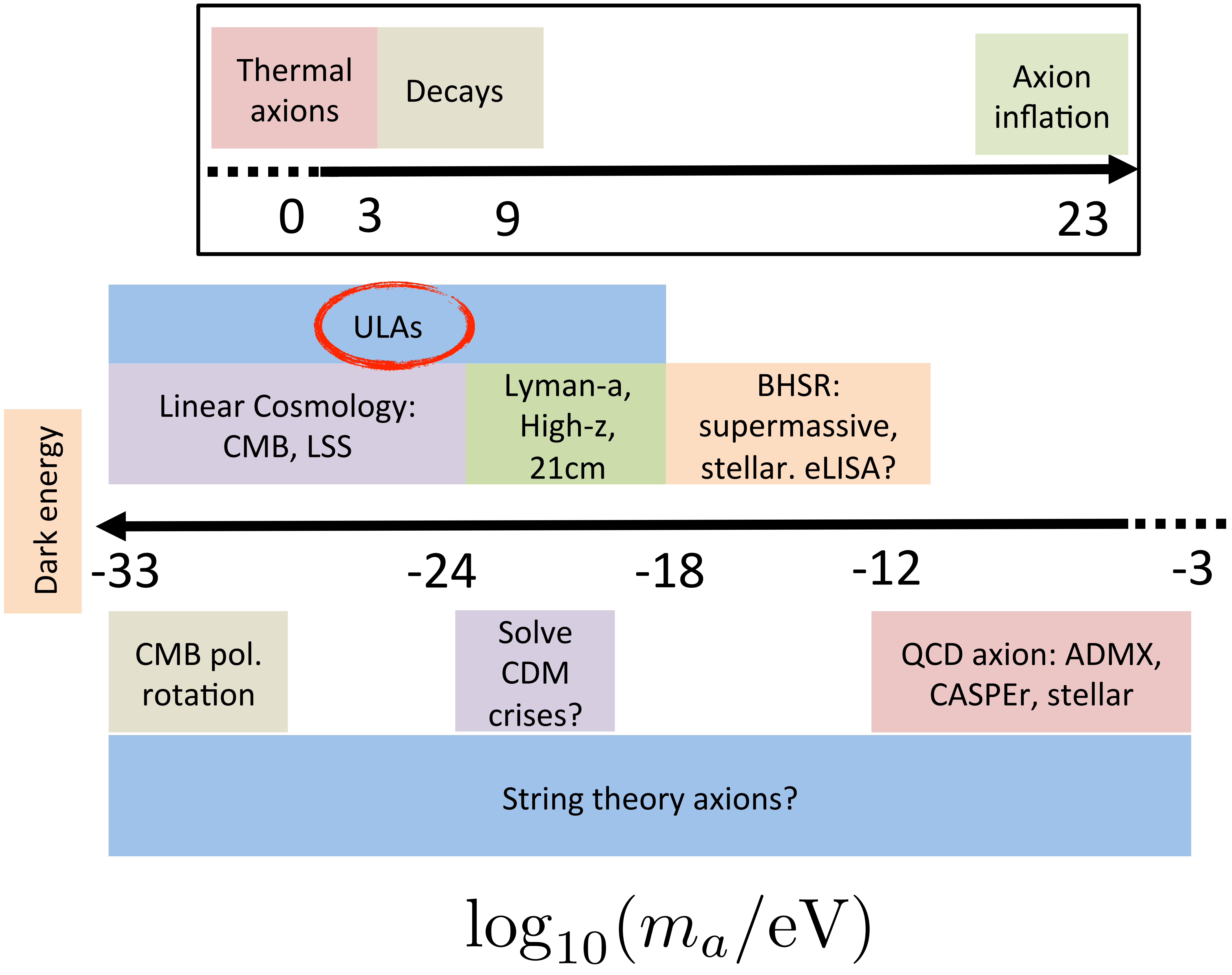

D. Marsh, Phys. Rept. 643, 1-79 (2016)

Physical properties of ALDM

- **Local ALDM field** made up by a large number of ALP classical fields with uncorrelated random phases Foster, Rodd, Safdi, PRD 97, no.12, 123006 (2018)

density **velocity element**

$$a(\mathbf{x},t) = \frac{\sqrt{\rho(\mathbf{x})}}{m_a} \sum_d \alpha_d \sqrt{f_{\mathbf{x}}(\mathbf{v}_d)(\Delta v)^3} \cos[\omega_a(t - \mathbf{v}_d \cdot \mathbf{x}) + \phi_d]$$

  - **Non-relativistic limit**: $\omega_a \approx m_a$; velocity distribution $f_{\mathbf{x}}(\mathbf{v})$ peaked around $|\mathbf{v}| \sim v_0 \sim 10^{-3}c$ (CDM velocity in our galaxy)
  - **Random nature**: random amplitude α_d and phase ϕ_d (follow the Rayleigh and uniform distributions)

- **ALPs effective action**: gravitational interaction, coupling to SM particles…

$$S = \int d^4x \sqrt{-g} \left[\frac{1}{2} \nabla^\mu a \nabla_\mu a - \frac{1}{2} m_a^2 a^2 + \frac{g_{a\gamma}}{2} a F_{\mu\nu} \tilde{F}^{\mu\nu} + \frac{g_{af}}{2m_f} \nabla_\mu a (\bar{f} \gamma^\mu \gamma_5 f) + ... \right]$$

Chern-Simons coupling

ALDM induced cosmic birefringence

Chern-Simons coupling g corrects the dispersion relations of two circular polarization modes of photons, yielding polarization angle (PA) rotation of linearly polarized photons

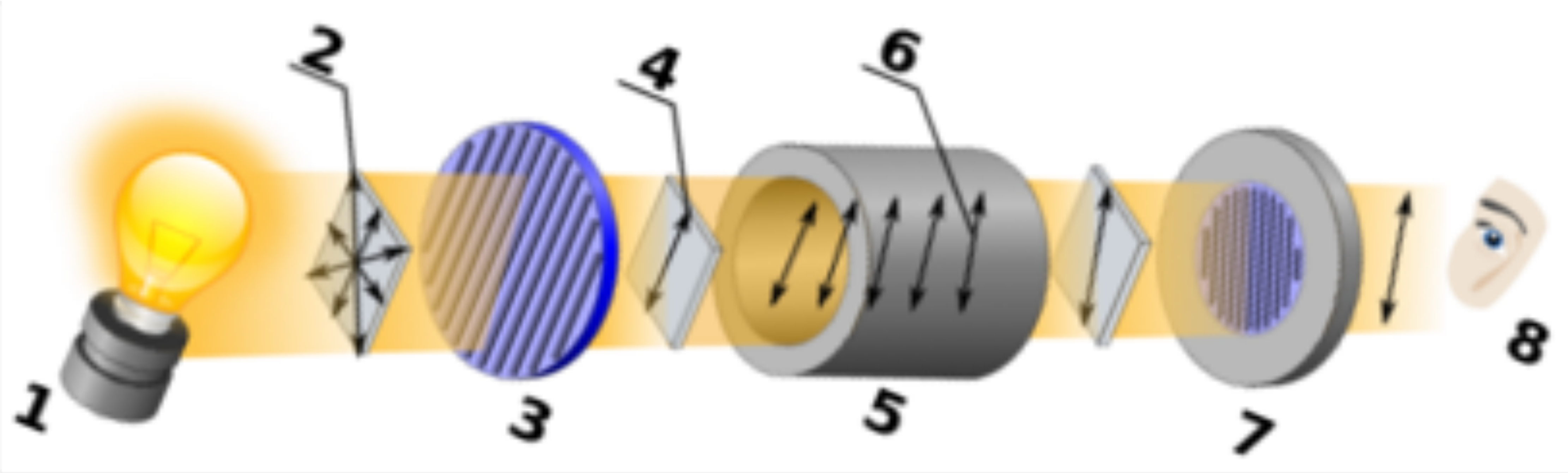

$$\omega_{\pm} \simeq k \pm g \left(\frac{\partial a}{\partial t} + \nabla a \cdot \frac{\mathbf{k}}{k} \right) = k \pm g\, n^{\mu} \nabla_{\mu} a$$

$$\Delta\theta_{p,n} \simeq -g \int_{C_{p,n}} ds\, n^{\mu}\, \nabla_{\mu} a(\mathbf{x}, t)$$ ($C_{p,n}$: the photon traveling path, n^{μ}: the null tangent vector to $C_{p,n}$)

$$\approx \frac{g}{m_a} \sum_d \alpha_d \Big\{ \underbrace{\sqrt{\rho_p f_p} \cos[m_a(t_n - L_p - \mathbf{v}_d \cdot \mathbf{x}_p) + \phi_d]}_{\text{"Pulsar"}} - \underbrace{\sqrt{\rho_e f_e} \cos(m_a t_n + \phi_d)}_{\text{"Earth"}} \Big\} (\Delta v)^{\frac{3}{2}} .$$

- relies only on field profiles at two endpoints of photon traveling
- quasi-monochromatic oscillation around the frequency $\omega_a \approx m_a$
- no frequency dependence (Faraday Rotation increases with wavelength)

Detection of cosmic birefringence

A variety of **astrophysical light sources** proposed to detect cosmic birefringence

- Carroll, Field, Jackiw, PRD 41, 1231 (1990)
- Antonucci, Ann. Rev. Astron. Astrophys. 31, 473 (1993).
- Ivanov, Kovalev, Lister, Panin, Pushkarev, Savolainen, Troitsky, JCAP 02, 059 (2019), 1811.10997
- Fujita, Tazaki, Toma, Phys. Rev. Lett. 122, 191101 (2019), 1811.03525
- Liu, Smoot, Zhao, Phys. Rev. D 101, 063012 (2020), 1901.10981.
- Caputo, Sberna, Frias, Blas, Pani, Shao, Yan, Physical Review D 100, 063515 (2019
- Chigusa, Moroi, Nakayama, Phys. Lett. B 803, 135288 (2020), 1911.09850.
- Chen, Shu, Xue, Yuan, Zhao, Phys. Rev. Lett. 124, 061102 (2020), 1905.02213
- …

PHYSICAL REVIEW D VOLUME 43, NUMBER 12 15 JUNE 1991

ARTICLES

Einstein equivalence principle and the polarization of radio galaxies

Sean M. Carroll and George B. Field
Harvard-Smithsonian Center for Astrophysics, Cambridge, Massachusetts 02138
(Received 26 December 1990)

Mainly focus on the **temporal oscillation** feature of the signal for individual sources;
spatial correlations among different sources not properly considered

PPA may provide an excellent tool to study the spatial correlations of cosmic birefringence induced by the ultralight ALDM

ALDM induced signal for PPAs

PA rotation signal on PPAs with many pulsars   Liu, Lou, **JR**, 2021, [arXiv: 2111.10615]

- Construct a **signal vector s** from the time series of PA rotation for each pulsar in PPA

$$\mathbf{s} \equiv (\Delta\theta_{1,1}, \ldots, \Delta\theta_{1,N_1}, \ldots, \Delta\theta_{\mathcal{N},1}, \ldots, \Delta\theta_{\mathcal{N},N_{\mathcal{N}}})^T$$

- Signal **s** follows a **multivariable Gaussian distribution** with zero mean and the covariance matrix

$$\Sigma^{(s)}_{p,n;q,m} \approx \frac{g^2}{m_a^2}\left\{\rho_e \cos(m_a \Delta t) + \sqrt{\rho_p \rho_q}\cos[m_a(\Delta t - \Delta L)]\frac{\sin y_{pq}}{y_{pq}} + \ldots\right\}$$

$y_{pq} = \Delta x / l_c$

$l_c = 1/(m_a v_0)$

(coherence length)

Comparison	SGWB	ALDM (PTAs and PPAs)
Earth-term correlation	quadrupolar correlation	monopolar correlation (universal)
pulsar-term correlation	pulsar-terms suppressed in $L \gg 1/\omega$ limit; spatial correlations rapidly degrade	spatial correlations degrade slower ($L \gg l_c \gg 1/m_a$); encode DM density dep.; enhanced at galactic center

Pulsar correlations

- Both **auto-correlation** of individual pulsars and **cross-correlation** among different pulsars contribute
- Cross-correlation highly valuable to distinguish spatial correlated and uncorrelated contributions

NANOGrav detectes oscillating PA rotation with period ~1yr, (2104.05723)

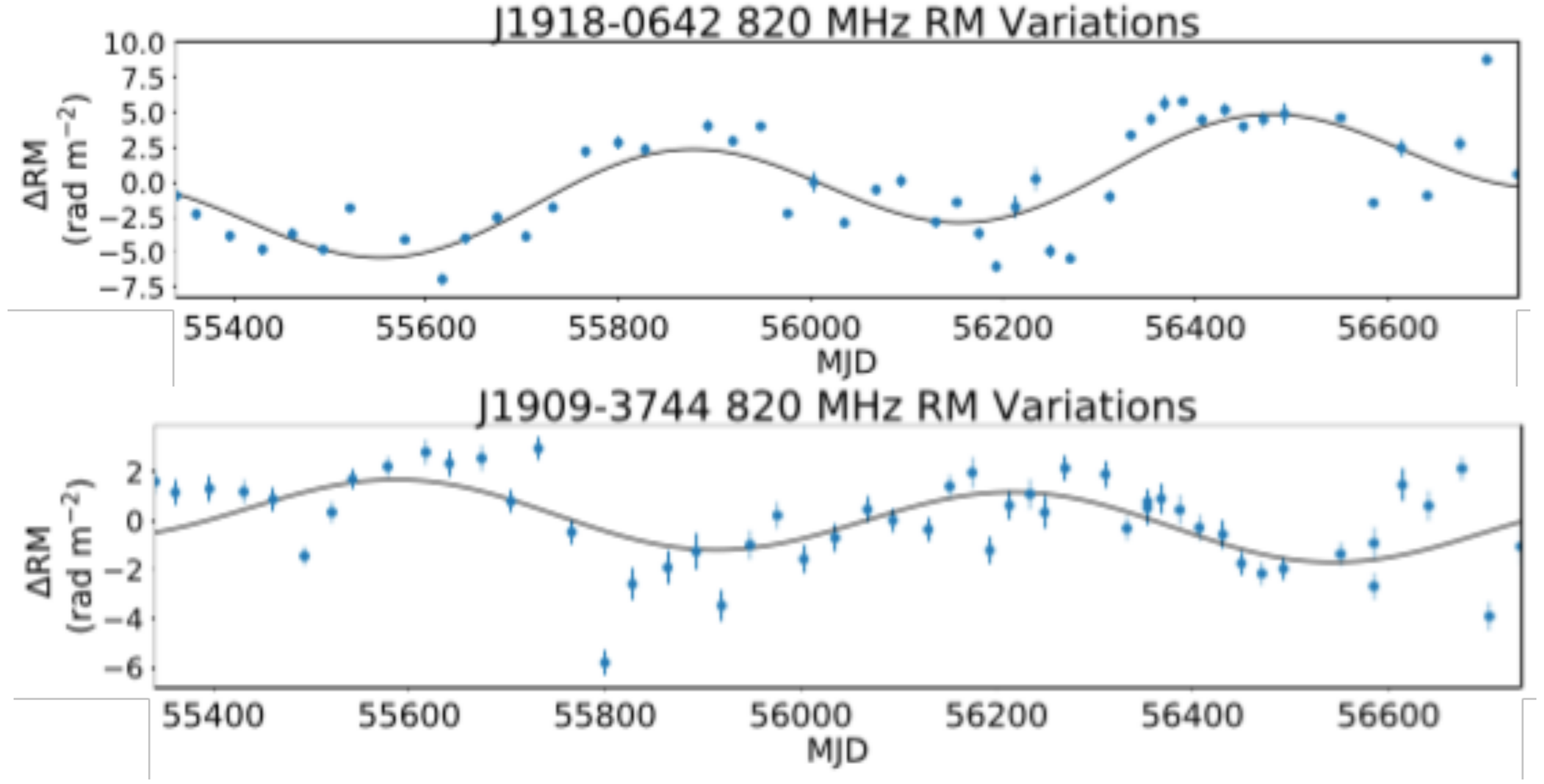

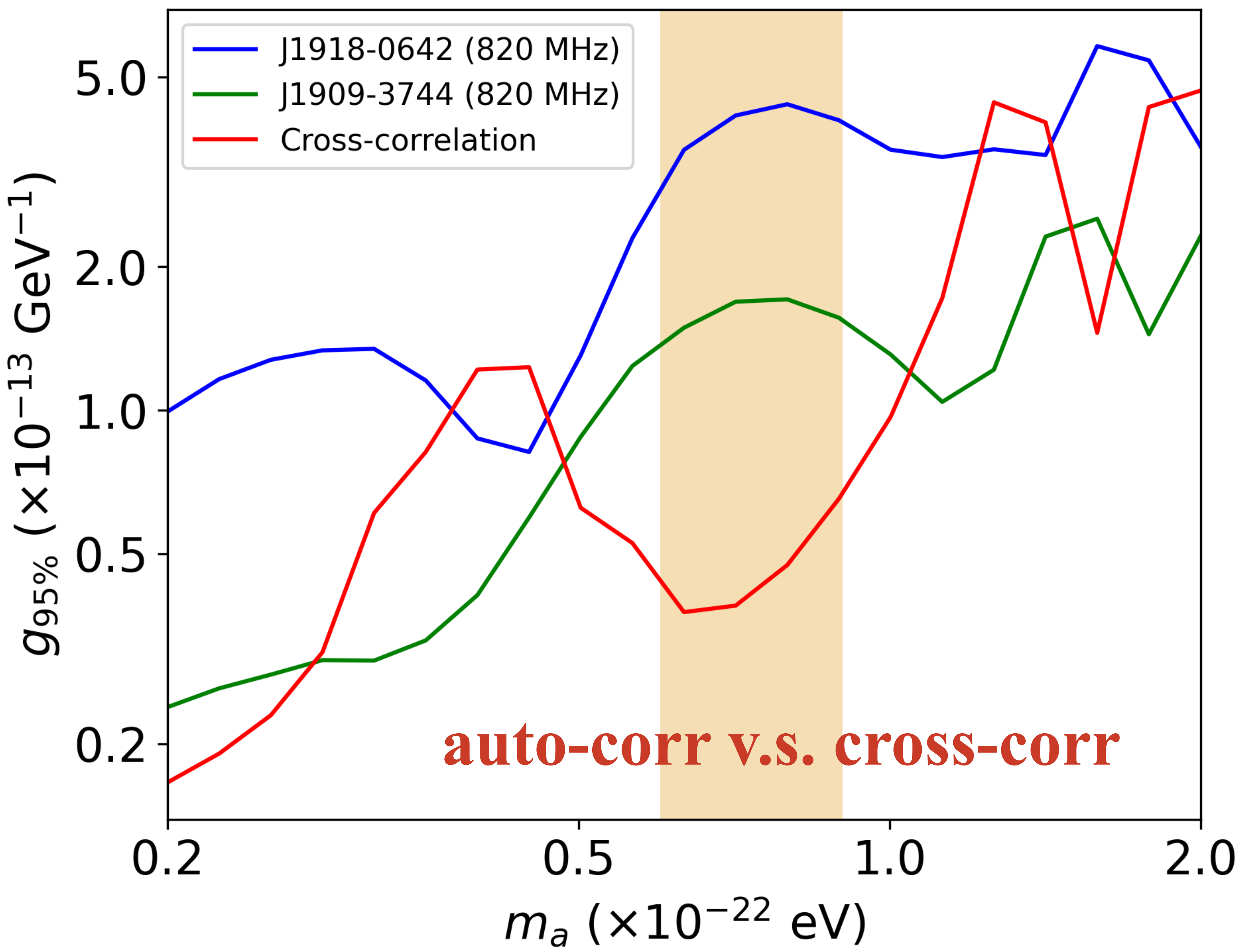

Likelihood function: $\mathcal{L}(\theta|\mathbf{d}) = \det[2\pi\mathbf{\Sigma}]^{-1/2} \exp\left[-\frac{1}{2}\mathbf{d}^T \cdot \mathbf{\Sigma}^{-1} \cdot \mathbf{d}\right]$, d = s + n (white), $\mathbf{\Sigma} = \mathbf{\Sigma}^{(s)} + \mathbf{B}$

Exclusion TS on the coupling g: $q(g, m_a) \equiv 2[\ln \mathcal{L}(\hat{g}, m_a|\mathbf{d}) - \ln \mathcal{L}(g, m_a|\mathbf{d})]$ ($\hat{g}$ maximizes likelihood)

Pulsar correlations

Asimov form of exclusion TS for projection: averaging different data realizations under the background only assumption

$$\langle q \rangle = \mathrm{Tr}\left[\mathbf{B}(\mathbf{\Sigma}^{-1} - \mathbf{B}^{-1})\right] + \ln\det\mathbf{\Sigma}/\ln\det\mathbf{B} + ...$$

$$\langle q \rangle \approx \frac{1}{2}\sum_{p,q}\frac{1}{\lambda_p\lambda_q}\mathrm{Tr}\left(\mathbf{\Sigma}^{(s)}_{pq}\mathbf{\Sigma}^{(s)}_{qp}\right)$$ (small signal limit; λ noise variance)

Auto-correlation

$$\mathrm{Tr}\left(\mathbf{\Sigma}^{(s)}_{pp}\mathbf{\Sigma}^{(s)}_{pp}\right) \sim \frac{g^4}{m_a^4}N_p^2\left[\rho_e + \rho_p - 2\sqrt{\rho_e\rho_p}\cos(m_a L_p)\frac{\sin y_{ep}}{y_{ep}}\right]^2. \quad y_{ep} = L_p/l_c$$

# of data points for p-th pulsar

- N_p enhancement reflects temporal correlation, **insensitive to distribution of sampled points**
- Earth-pulsar correlation (3rd) suppressed if $L_p \gg l_c$

Cross-correlation

$$\mathrm{Tr}\left(\mathbf{\Sigma}^{(s)}_{pq}\mathbf{\Sigma}^{(s)}_{pq}\right) \sim \frac{g^4}{m_a^4}N_pN_q\left[\rho_e^2 + \rho_p\rho_q\frac{\sin^2 y_{pq}}{y_{pq}^2} + 2\rho_e\sqrt{\rho_p\rho_q}\cos(m_a\Delta L)\frac{\sin y_{pq}}{y_{pq}} + f(y_{ep}, y_{eq})\right].$$

- Earth-terms cross-correlations (1st) universal
- Pulsar-terms cross-correlations (2nd) dominate for pulsars around galactic center

PPA projected sensitivity to ALDM

- Three PPA scenarios (different stage of PTAs)

  NPPA: 100 MSPs around 1kpc (*current PTAs*)

  FPPA: 100 MSPs in galactic bulge (*FAST/SKA era*)

  OPPA: 100 MSPs following ATNF (*FAST/SKA era*)

- **Galactic ALDM density profile**: soliton formed by quantum pressure ($r < l_c$, $\rho_c \propto m_a^2$) + NFW ($r > l_c$); CMB constraints on relic abundance imposed

- **Pulsar distance uncertainty** (~20%) marginalized in constraints estimate

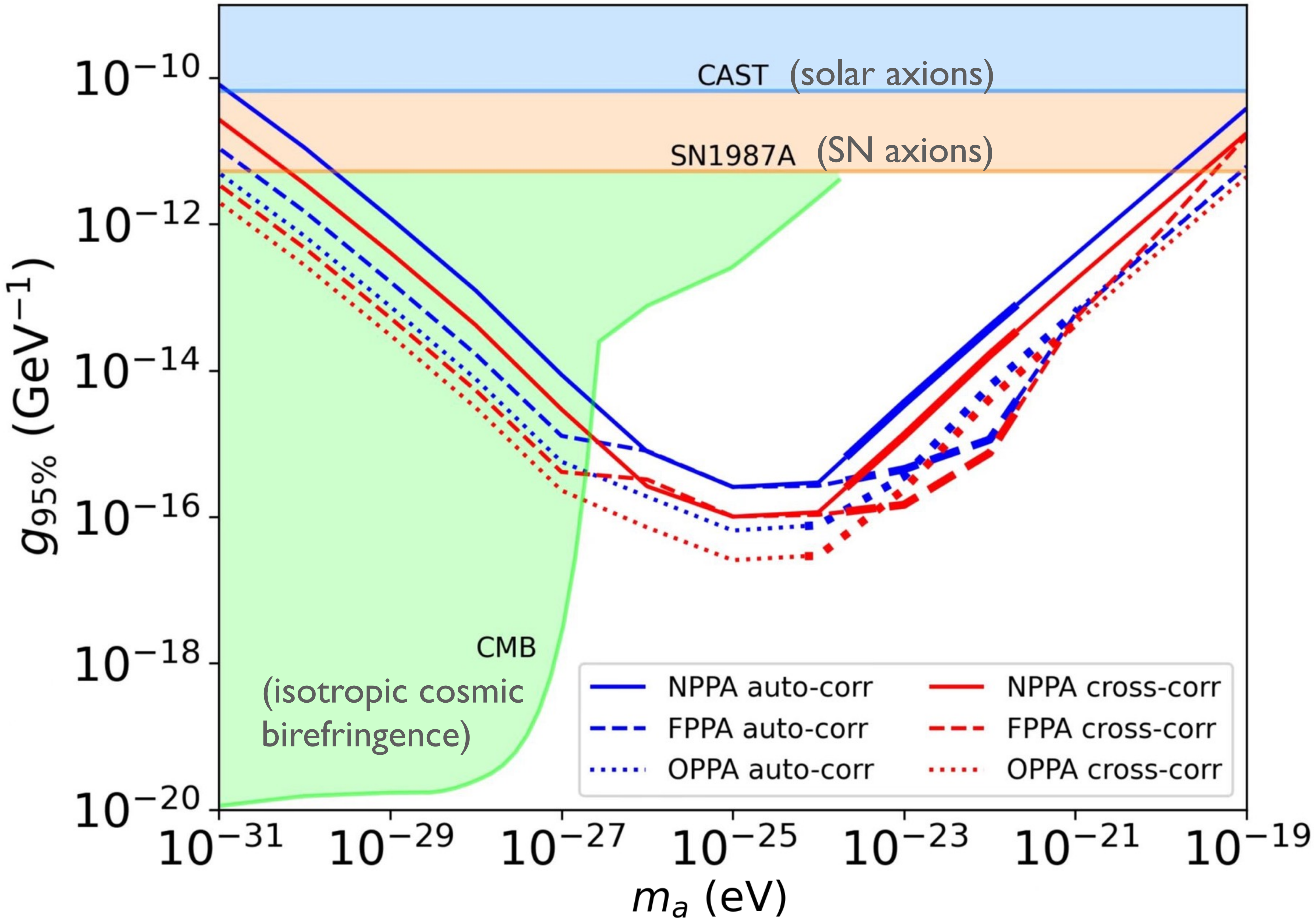

- **Cross-correlation limits** are typically **stronger** than auto-correlation ones
- As m_a decreases, the limit decreases (fuzzy DM), stay flat and increases
- Projected PPA limits form a great complementarity with the existing bounds

Ultralight ALDM induced timing signal

- **PTA signal:** temporal oscillation of scalar field induces temporal oscillating gravitational potential and then changes the pulse time of arrival (TOA) Khmelnitsky, Rubakov, 2014 [JCAP]

$$\Delta t(t) = -\int_0^t \frac{\Omega(t') - \Omega_0}{\Omega_0} dt' = \underbrace{\frac{\Psi_c(x_e)}{2\pi f}\sin[2\pi f t + 2\alpha(x_e)]}_{\text{"Earth"}} - \underbrace{\frac{\Psi_c(x_p)}{2\pi f}\sin\left[2\pi f\left(t - \frac{d_p}{c}\right) + 2\alpha(x_p)\right]}_{\text{"Pulsar"}}$$

$$f = \frac{2m}{2\pi} = 4.8\times 10^{-8}\left(\frac{m}{10^{-22}\mathrm{eV}}\right)\mathrm{Hz}$$

$$\Psi_c = \frac{G\rho_{\mathrm{SF}}}{\pi f^2} \approx 6.1\times 10^{-18}\left(\frac{m}{10^{-22}\,\mathrm{eV}}\right)^{-2}\left(\frac{\rho_{\mathrm{SF}}}{0.4\,\mathrm{GeV\,cm^{-3}}}\right)$$

- **PTA limits:** current limits from PPTA too weak to constrain ultralight scalar DM; forecasted limits improved (lower noise, more pulsars, more data…)

$$\delta t \approx 0.02\,\mathrm{ns}\left(\frac{m}{10^{-22}\,\mathrm{eV}}\right)^{-3}\left(\frac{\rho_{\mathrm{SF}}}{0.4\,\mathrm{GeV\ cm^{-3}}}\right)$$

(timing residual amplitude >20 ns for m < 10^{-23} eV)

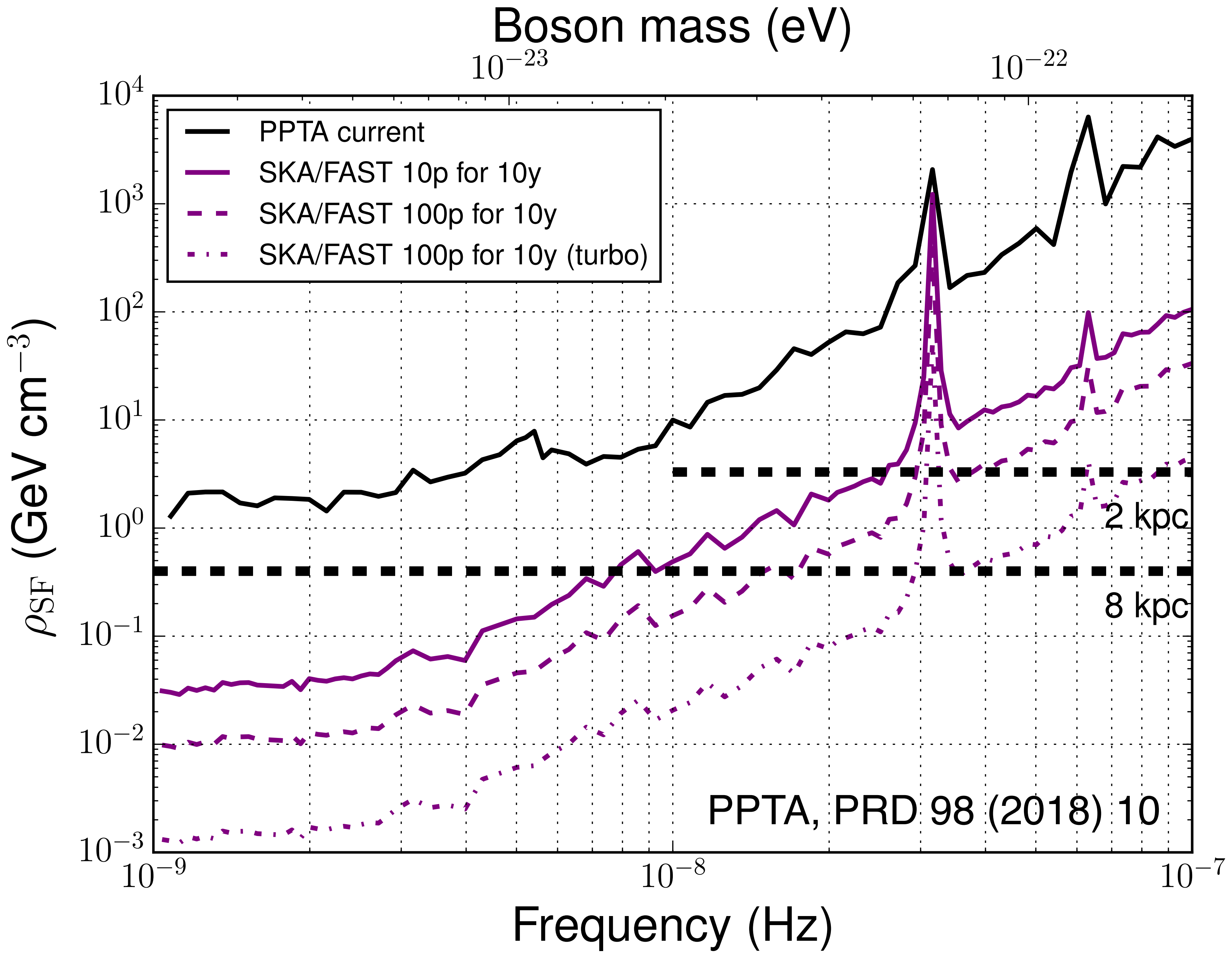

Cross-correlation of PTA and PPA

- Stochastic description for both TOA and PA rotation

$$\Delta\theta_{p,n} = \frac{g}{m_a}\sum_{\mathbf{v}} \alpha_{\mathbf{v}}\sqrt{f(\mathbf{v})}(\Delta v)^{\frac{3}{2}} \sum_{i=0,1}(-1)^i\sqrt{\rho(\mathbf{x}_p^{(i)})}\cos\left[m_a t_{p,n}^{(i)} - m_a \mathbf{v}\cdot\mathbf{x}_p^{(i)} + \phi_{\mathbf{v}}\right]$$ (linear in ALDM field)

$$\Delta t_{p,n} = \frac{\pi G}{4m_a^3}\sum_{\mathbf{v},\mathbf{v}'} \alpha_{\mathbf{v}}\alpha_{\mathbf{v}'}\sqrt{f(\mathbf{v})f(\mathbf{v}')}(\Delta v\Delta v')^{\frac{3}{2}} \sum_{i=0,1}(-1)^i\rho(\mathbf{x}_p^{(i)})\sin\left[2m_a t_{p,n}^{(i)} - m_a(\mathbf{v}+\mathbf{v}')\cdot\mathbf{x}_p^{(i)} + \phi_{\mathbf{v}} + \phi_{\mathbf{v}'}\right]$$

(quadratic in ALDM field)

$$\langle\Delta\theta_{p,n}\Delta\theta_{q,m}\rangle = \frac{g^2}{m_a^2}\sum_{i,j=0,1}(-1)^{i+j}\sqrt{\rho(\mathbf{x}_p^{(i)})\rho(\mathbf{x}_q^{(j)})}\cos\left[m_a(t_{p.n}^{(i)} - t_{q,m}^{(j)})\right]\frac{\sin y_{pq}^{(ij)}}{y_{pq}^{(ij)}}.$$ **(PPA covariance matrix)**

$$\langle\Delta t_{p,n}\Delta t_{q,m}\rangle = \left(\frac{\pi G}{2m_a^3}\right)^2\sum_{i,j=0,1}(-1)^{i+j}\rho(\mathbf{x}_p^{(i)})\rho(\mathbf{x}_q^{(j)})\cos[2m_a(t_{p,n}^{(i)} - t_{q,m}^{(j)})]\left(\frac{\sin y_{pq}^{(ij)}}{y_{pq}^{(ij)}}\right)^2$$ **(PTA covariance matrix)**

Cross-correlation of PTA and PPA

- Stochastic description for both TOA and PA rotation

$$\Delta\theta_{p,n} = \frac{g}{m_a}\sum_{\mathbf{v}} \alpha_{\mathbf{v}} \sqrt{f(\mathbf{v})}(\Delta v)^{\frac{3}{2}} \sum_{i=0,1}(-1)^i \sqrt{\rho(\mathbf{x}_p^{(i)})} \cos\left[m_a t_{p,n}^{(i)} - m_a \mathbf{v}\cdot\mathbf{x}_p^{(i)} + \phi_{\mathbf{v}}\right]$$

(linear in ALDM field)

$$\Delta t_{p,n} = \frac{\pi G}{4m_a^3}\sum_{\mathbf{v},\mathbf{v}'} \alpha_{\mathbf{v}}\alpha_{\mathbf{v}'} \sqrt{f(\mathbf{v})f(\mathbf{v}')}(\Delta v \Delta v')^{\frac{3}{2}} \sum_{i=0,1}(-1)^i \rho(\mathbf{x}_p^{(i)}) \sin\left[2m_a t_{p,n}^{(i)} - m_a(\mathbf{v}+\mathbf{v}')\cdot\mathbf{x}_p^{(i)} + \phi_{\mathbf{v}} + \phi_{\mathbf{v}'}\right]$$

(quadratic in ALDM field)

- Cross-correlation of TOA and PA rotation   Liu, **JR**, Xu, 2021, ongoing…

$\langle \Delta t_{p,n}\Delta\theta_{q,m}\rangle = 0$ due to non-cancellation of the random phases

$$\langle \Delta\theta_{p,n}\Delta\theta_{q,m}\Delta t_{r,l}\rangle = -\frac{\pi G g^2}{4m_a^5}\sum_{i,j,k=0,1}(-1)^{i+j+k}\rho(\mathbf{x}_r^{(k)})\sqrt{\rho(\mathbf{x}_p^{(i)})\rho(\mathbf{x}_q^{(j)})}$$
$$\times \sin\left[m_a(2t_{r,l}^{(k)} - t_{p,n}^{(i)} - t_{q,m}^{(j)})\right] \frac{\sin y_{rp}^{(ki)}}{y_{rp}^{(ki)}} \frac{\sin y_{rq}^{(kj)}}{y_{rq}^{(kj)}}.$$

(leading order contribution)

Summary and Outlook

- We propose **development of PPAs** with the same data acquired for PTAs. PPAs can be used to **detect ultralight ALDM induced cosmic birefringence with special temporal and spatial correlations**. Projected limits on its Chern-Simons coupling form a great complementarity with existing bounds

- Real data analysis with PPTA polarization data

  Liu, Luu, **JR**, Shu, Xue, Zhao 2022, ongoing…

- Cross-correlation of ALDM-induced signals on PPAs and PTAs

  Liu, **JR**, Xu, 2022, ongoing…

- More physical targets for PPAs as a new tool for exploring fundamental physics?

- Synergize PPAs with other observations to further distinguish different scenarios?

Thank You!